ТЕХНІКА ТА МЕТОДИ ЕКСПЕРИМЕНТУ
ENGINEERING AND METHODS OF EXPERIMENT

УДК 539.166+539.12-17 https://doi.org/10.15407/jnpae2022.04.280

M. A. El-Sarraf[1,*], A. A. El-Sayed Abdo[2]

[1] *Nuclear and Radiological Safety Research Center, Egyptian Atomic Energy Authority, Cairo, Egypt*
[2] *Nuclear Research Center, Egyptian Atomic Energy Authority, Cairo, Egypt*

*Corresponding author: magdsarraf@yahoo.com

EVALUATION OF GAMMA-RAY BUILDUP FACTORS FOR SOME WASTE PAPER AND NATURAL RUBBER COMPOSITES

In this work, four waste paper composites were studied in terms of several photon interaction parameters over the energy region from 0.015 to 15.0 MeV. The waste paper and natural rubber (WP/NR) composites of different densities ranging from $\rho = 0.894$ to 1.16 gm·cm^{-3} were used for shielding radioactive rubble at different time period stages. Some additives were also used including high-abrasion furnace black, paraffin wax, B_4C, as well as magnetite. The deduced parameters of photon interaction: equivalent atomic number Z_{eq}, exposure buildup factor and energy absorption buildup factor have been studied as a function of incident photon energy, WP/NR elemental composition, and for penetration depths, up to 40 mean free path. The Z_{eq} numbers have shown slight variation over the selected incident energy range and buildup factors were found to be modest at low and high photon energy meanwhile their values increase widely over the intermediate energy region. In addition, kerma relative to air for photon energies from 1 to 20 MeV were computed and show dependence upon equivalent atomic numbers. In this work, it was clear that filled samples offer better shielding capabilities than unfilled ones. The obtained data could be useful for radiation physicists and scientists in estimating the γ-irradiation received after applying such shields.

Keywords: composites, buildup factors, exposure, energy absorption, kerma.

1. Introduction

In a Nuclear Power Station accident, large amounts of radioactive rubble result and make their shielding process, either temporarily or permanently, a requirement for protection against harmful emissions [1, 2].

In previous studies, sheets of waste paper and natural rubber (WP/NR) were designed and tested to be used for radiation shielding for different purposes [3, 4].

Since massive rubble is a source of large amounts of radiation, comprehensive γ-ray reaction data is required for overall shielding calculations [5].

Generally, the most basic radiation interaction parameter is the linear attenuation coefficient μ which is applied through the well-known Beer - Lambert equation. However, for this, strict conditions such as thin uniform investigated target material should apply. To avoid dependency on density we can choose to divide μ by density ρ and obtain the so-called mass attenuation coefficient.

In fact, the γ-attenuation process deviates from this law according to multiple photon scattering and we had to submit a correction named the buildup factor *B*. This factor comes up, especially upon Compton scattering. Further, the energy of incident photons reduces and they change their direction before being reflected by the receiver. This *B* is vital for attenuation calculations and can affect its quality [6 - 9].

As γ-rays impinge on shielding material, we would expect two components within or beyond the material; the collided and the non-collided photons. The *B* could be regarded as the ratio of the first to the second component at the concerning point of observation [10 - 12].

This facto could be expressed in two terms: first – exposure buildup factor (EBF) in which the quality of interest is exposure, and energy response function is that of absorption in the air; second – energy absorption buildup factor (EABF) in which the absorbed or deposited energy is in the shielding medium and the response function is that of absorption in the material [8].

First, and in order to account for such photon interaction parameters, mass attenuation coefficient μ/ρ and mean free path (mfp) were evaluated with the help of the state-of-the-art WinXCom software package [13, 14].

In addition, and as a step for B computation, equivalent atomic numbers Z_{eq} which describe the composite material in terms of elements should be presumed.

Since the 1950s, different works provided a number of empirical formulas for the computation of buildup factors. In recent times, tools like the geometric-progression (GP) fitting method and others like the invariant embedding method have been utilized [11, 15 - 21].

In the present work, the EBF and EABF for four WP/NR composites will be evaluated using the GP fitting method in the energy range from 0.015 to 15 MeV and from 5 to 40 mfp using equations and parameters given by (ANSI/ANS-6.4.3-1991) [5]. This standard presents evaluated γ-ray buildup factors for materials used in shielding calculations of structures in power plants and other nuclear facilities.

Also, kerma values, which describe released kinetic energy in samples, will be demonstrated [22 - 25].

In case of any nuclear accident, such as Fukushima-Daiichi in Japan, this study will definitely help radiation health physicists and engineers of rubble storage facilities in dosimetry calculations of effective radiation coming out of the selected protective shields. This could be achieved by computing the dose that can affect the indoor people residing in buildings constructed near rubble storage facilities.

2. Computational procedure

The used chemical composition and densities of WP/NR samples are given in Table 1.

Table 1. **Samples of WP/NR mixes, phr**

Composite ingredients, phr	S1 ρ = 0.894 g·cm^{-3}	S5 ρ = 1.16 g·cm^{-3}	S9 ρ = 1.044 g·cm^{-3}	S14 ρ = 0.99 g·cm^{-3}
Natural Rubber	100	100	100	100
Stearic Acid	2	2	2	2
HAF black	40	40	40	40
Processing Oil	10	10	10	10
B4C	20	20	20	0
Paraffin Wax	60	6	18	60
Waste Paper	0	54	0	0
Waste Paper/Magnetite	0	0	42	20
MBTS	2	2	2	2
P β N	1	1	1	1
ZnO	5	5	5	5
S	2	2	2	2

N o t e. ρ – density.

In order to calculate the mass attenuation coefficient μ/ρ, WinXCom was used, which is basically the XCom program transformed into the Windows platform [13, 14]. Another parameter, mean free path, is the reciprocal of the linear attenuation coefficient that could be deduced by then. The EBF and EABF computations are treated step by step as (i) calculation of equivalent atomic number Z_{eq}, then (ii) computation of five terms geometric progression parameters GP and followed by (iii) calculation of both buildup factors.

In our study, and since this phenomenon is a direct response to scattering, the Compton partial attenuation coefficient μ_{comp} and total attenuation coefficient μ_{tot} in cm^2·gm^{-1} were first obtained for elements of $Z = 1$ to 40 and for the concerned WP/NR samples as Z_{eq} for such samples would not exceed this value. We will also be using WinXCom over the energy range from 0.015 to 15 MeV.

The μ_{comp}/μ_{tot} ratio for all in-range elements and the samples was obtained, thus the value of Z_{eq} for WP/NR samples were deduced by matching the nominated ratio of a particular sample at selected energy with the corresponding ratio of an element at the same energy.

In case, WP/NR ratio lies between two known element ratios, we use the following interpolation formula

$$Z_{eq} = \frac{Z_1\left(\log R_2 - \log R\right) + Z_2\left(\log R - \log R_1\right)}{\log R_2 - \log R_1}, \quad (1)$$

where Z_1 and Z_2 are atomic numbers, before and after the suitable element, which correspond to the deduced ratios R_1 and R_2. In addition to that, R is the ratio for the selected WP/NR samples at each specific energy.

As for step (ii), the standard reference (ANSI/ANS-6.4.3-1991) provides the five (*b*, *c*, *a*, X_K, and *d*) GP fitting parameters *P*'s for different elements. Knowing Z_{eq} for each WP/NR sample, these factors will be computed by a similar interpolation formula to compute each prime value *P*.

$$P = \frac{P_1\left(\log Z_2 - \log Z_{eq}\right) + P_2\left(\log Z_{eq} - \log Z_1\right)}{\log Z_2 - \log Z_1}. \quad (2)$$

In the third step (iii), and depending on values obtained from step (ii), EBF and EABF for the investigated composites will be computed over 0.015 to 15.0 MeV and up to 40 mfp using the following formula given by [8, 17, 18, 26, 27]

$$B(E, x) = 1 + \frac{b-1}{K-1}\left(K^x - 1\right) \qquad \text{for K} \neq 1,$$

$$B(E, x) = 1 + (b-1)x \qquad \text{for K} = 1,$$

where

$$K(E, x) = cx^a + d\,\frac{\tanh\left(x / X_k - 2\right) - \tanh(-2)}{1 - \tanh(-2)}$$

$$\text{for } x \leq 40 \text{ mfp.} \qquad (3)$$

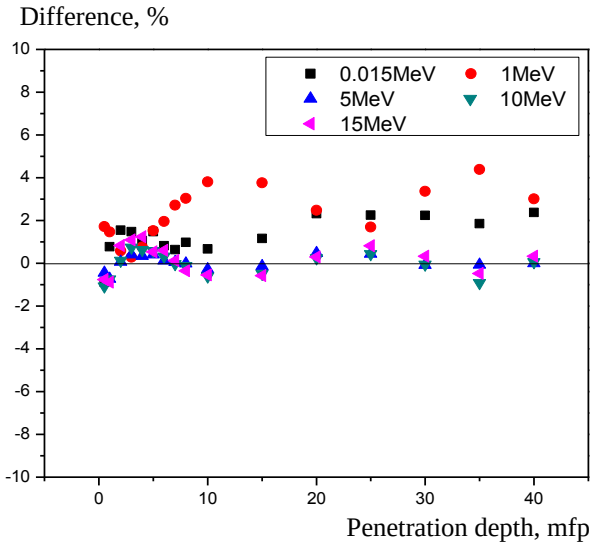

Fig. 1. Difference between air EBF as calculated by the developed method and the ANSI/ANS standard. (See color Figure on the journal website.)

From the comparison in Figs. 1 and 2, we can find our method to be very close to the standards with fair uncertainty, which provides confidence in our work for the selected samples [17, 28].

2.2. Computation of kerma relative to air

Kerma is the acronym for kinetic energy released in material, per unit mass, at the point of concern by un-charged radiations [29, 30]. These radiation types can be γ- and x-ray, etc., and kerma is in terms of the absorbed dose of the unit (J Kg^{-1} = Gy).

In addition, to calculate kerma relative to air for our samples, we can use the following relation;

$$K_a = K(\text{WP/NR})/K(\text{air}) = (\mu_{en}/\rho)(\text{WP/NR})/(\mu_{en}/\rho)(\text{air}). \qquad (4)$$

The mass energy absorption coefficients, μ_{en}/ρ for both samples and air are calculated using the compounding rule:

$$\mu_{en}/\rho = \Sigma_i\, w_i\, (\mu_{en}/\rho)_i, \qquad (5)$$

where w_i and $(\mu_{en}/\rho)_i$ are the weight fraction and mass-energy absorption coefficient for *i*-th constituting element, respectively.

The μ_{en}/ρ values for composite elements as well as air are taken from Ref. [31].

2.1 Validity of the procedure

To check the validity of the calculated values of EBF and EABF of our work for WP/NR composites, the used tool was applied for air and compared with those presented by (ANSI/ANS-6.4.3-1991) at the same media (air) over the investigated energy region and up to penetration depth of 40 mfp.

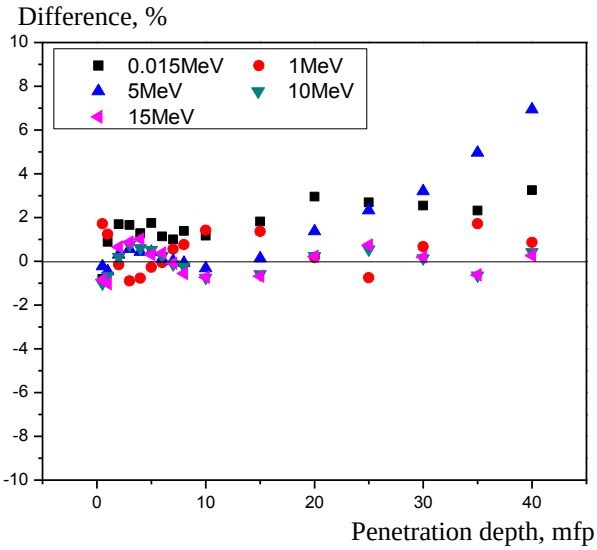

Fig. 2. Difference between air EABF as calculated by the developed method and the ANSI/ANS standard. (See color Figure on the journal website.)

3. Results and discussion

3.1 Equivalent atomic number

The equivalent atomic numbers Z_{eq} of the concerned WP/NR samples, namely, blank sample S1 and filled samples S5, S9, and S14 were calculated at the photon energy range from 0.015 to 15 MeV and are presented in Table 2.

The values of Z_{eq} will describe the sample in terms of equivalent elements that resemble the atomic number of a proposed single element.

As it is known, the interaction process of photons with matter is through photo absorption, Compton scattering, and pair production. These reactions are energy dependent.

Since Z_{eq} is calculated on the basis of Compton scattering, the slight variation in its value with photon energy could be explained in terms of Compton scattering cross-section variation upon energy.

From Table 2, it is clear that the filled samples have higher Z_{eq} values rather than the unfilled blank sample. In addition, Z_{eq} values in both cases individually, either for the blank or filled group, are very close and at all the incident photon energies. This behavior is due to the close elemental composition of all samples.

Additionally, it is found that S14 does have the highest values of Z_{eq} despite its marginally low density among filled samples. This could be attributed to its higher light element content.

Table 2. **Equivalent atomic numbers of the investigated samples**

E, MeV	Equivalent atomic number (Z_{eq})			
	S1	S5	S9	S14
0.015	8.148383	8.792437	8.577889	9.934359
0.02	8.332222	8.99234	8.772521	10.19246
0.03	8.517072	9.213159	8.982719	10.46475
0.04	8.582286	9.294827	9.064433	10.58006
0.05	8.585565	9.307379	9.076661	10.61602
0.06	8.555386	9.678168	9.054294	10.60779
0.08	8.440702	9.178943	8.942305	10.5116
0.1	8.306674	9.0483	8.789126	10.36896
0.15	8.00316	8.677204	8.431513	9.990297
0.2	7.730538	8.395301	8.169308	9.656017
0.3	7.405771	8.048731	7.815148	9.231348
0.4	7.236409	7.834963	7.609377	8.997781
0.5	7.14005	7.708715	7.493186	8.83822
0.6	7.083721	7.634048	7.424725	8.743387
0.8	7.031331	7.564136	7.360736	8.653981
1	7.016104	7.545057	7.342944	8.629189
1.5	6.054436	6.414023	6.256274	7.199701
2	5.69395	5.958539	5.829154	6.520302
3	5.608447	5.844079	5.724242	6.345433
4	5.588152	5.817404	5.699592	6.304415
5	5.580676	5.806677	5.690044	6.286921
6	5.575287	5.799342	5.683384	6.275442
8	5.569774	5.791695	5.676469	6.263857
10	5.567364	5.787352	5.672932	6.257057
15	5.562601	5.781454	5.66732	6.24601

3.2 Interpolation of EBF and EABF with incident photon

The EBF and EABF relation with photon energy was computed at energy range from 0.015 to 15 MeV and at fixed penetration depths of 1, 5, 10, 25, and 40 mfp. This variation was illustrated for the concerned samples S1, S5, S9, and S14; they are displayed in Figs. 3 - 6.

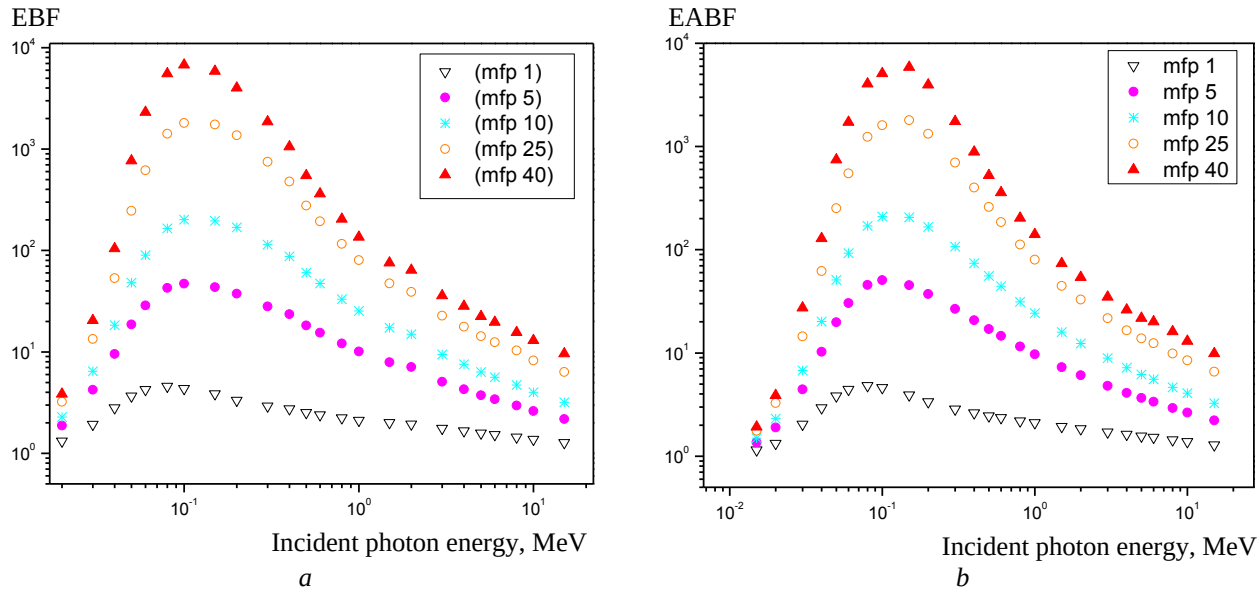

a *b*

Fig. 3. *a* – Variation of EBF for S1 with incident photon energy.
b – Variation of EABF for S1 with incident photon energy.
(See color Figure on the journal website.)

From the two groups of Figs. 3, *a*; 4, *a*; 5, *a*; 6, *a* and Figs. 3, *b*; 4, *b*; 5, *b*; 6, *b* for both kinds of buildup factors, which are basically considered for multiple scattering, we can realize the initial values close to unity at γ-energy 0.015 MeV. Afterward, and as energy increases, the buildup factors are greater than 1 for

all sample thicknesses, i.e., mean free paths, which is in clear violation of Beer - Lambert's law. The *B* values reach the apex and drop again. In general, all curves apply the same trend and fluctuation over the studied energy range.

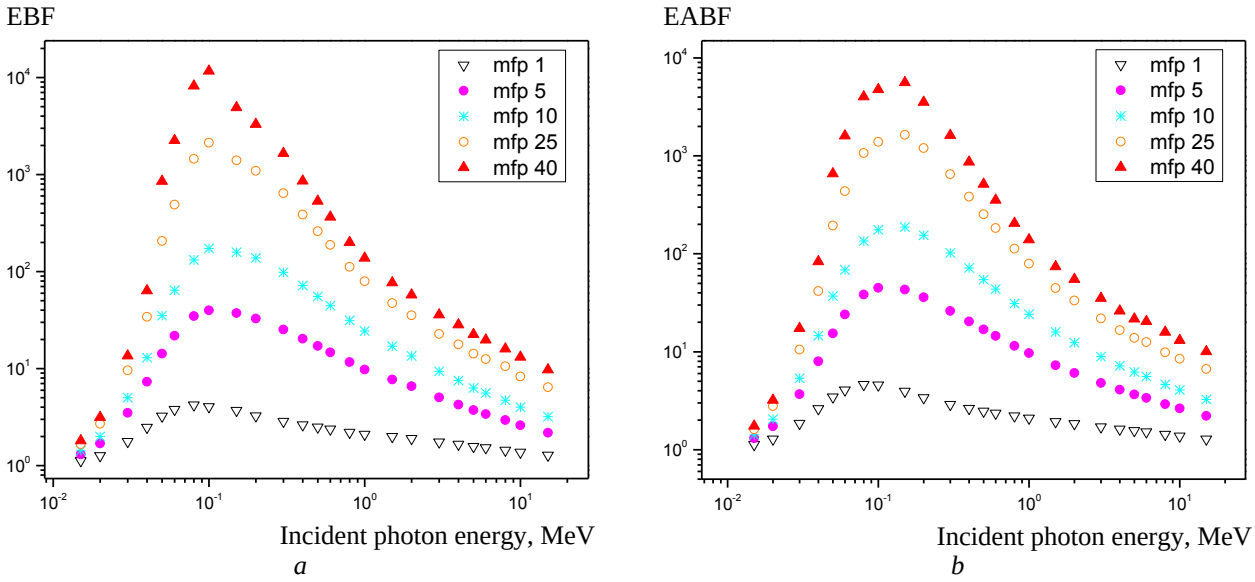

a *b*

Fig. 4. *a* – Variation of EBF for S5 with incident photon energy. *b* – Variation of EABF for S5 with incident photon energy. (See color Figure on the journal website.)

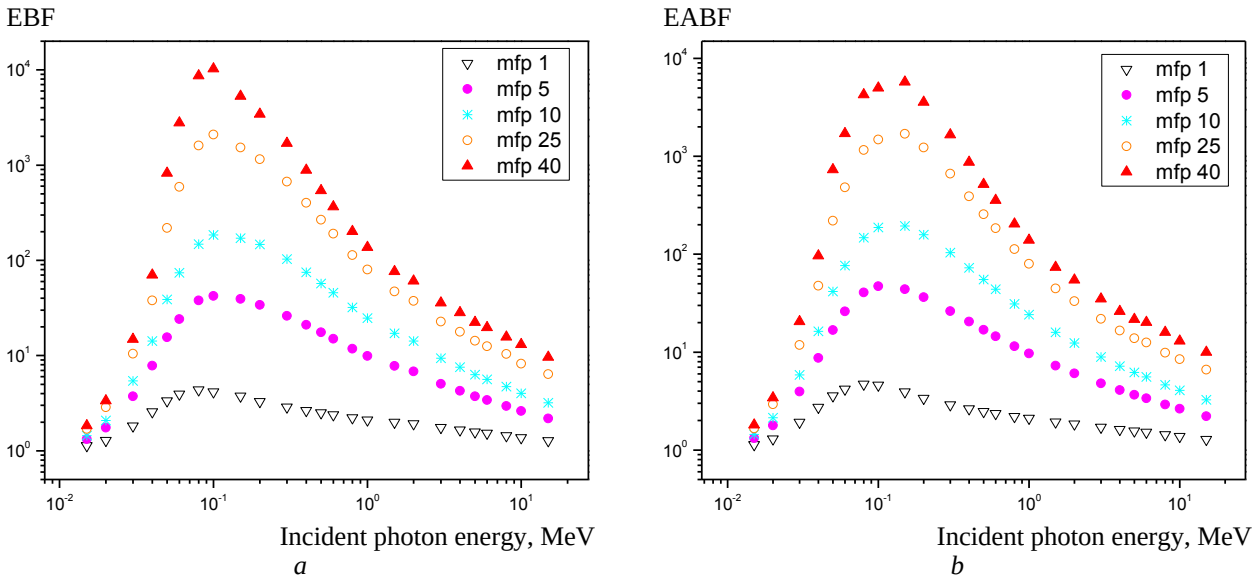

a *b*

Fig. 5. *a* – Variation of EBF for S9 with incident photon energy. *b* – Variation of EABF for S9 with incident photon energy. (See color Figure on the journal website.)

For the group of Figs. 3, *a*; 4, *a*; 5, *a*; 6, *a*, and in general, the buildup starts increasing moderately over low energies, where photoelectric absorption is the dominant interaction, and atomic cross-section is directly proportional to Z^{4-5}/E^{3-4}.

The photoelectric effect is considered a high agent for photons' removal and *B* values are minimum.

And as energy increases reaching an intermediate range, Compton multiple scattering dominates making *B* values reach high levels. Simply, because photons are not absorbed, however, their energies will be degraded.

This interaction overtakes at start energy called Photoelectronic-Compton, at which photoelectric matches Compton scattering. This reaction depends on Z^2.

Afterward, there is a decrease again in *B*'s, where photon energies increase above 1.02 MeV. At this level, we come to the renowned pair production region which is *Z* and Log (*E*) dependent.

Also, it is shown that for higher thicknesses (25 and 40 mfp), a relatively lower declension at buildup exists. Since the pair production process is actually a positron/electron production term, thicknesses give them greater chance for movement in samples, before finally being annihilated producing photons again.

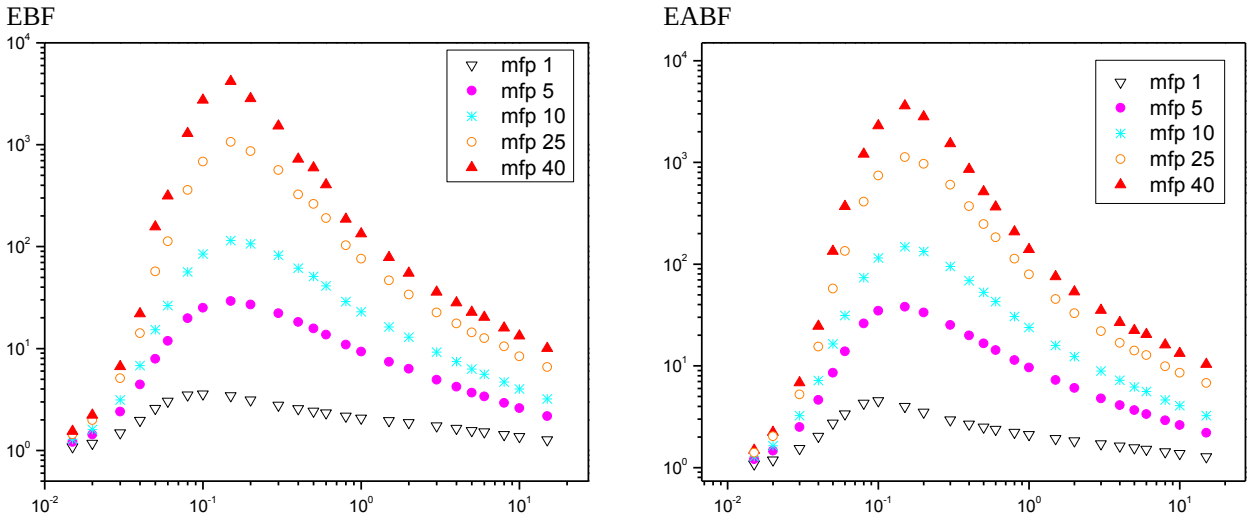

Fig. 6. *a* – Variation of EBF for S14 with incident photon energy. *b* – Variation of EABF for S14 with incident photon energy. (See color Figure on the journal website.)

This movement subsequently adds to the net photons economy and tries to bring the *B*'s up again.

For Figs. 3, *a*; 4, *a*; 5, *a* and 6, *a* individually, we can realize a shift of peaks towards higher energies as mean free paths increases. This could be explained according to different kinds of reactions.

Likewise, we can find a positive x-axis movement of peaks for the filled samples rather than the unfilled sample.

Upon comparing the height of peaks for filled samples S5, S9, and S14 to the unfilled S1 sample in total, we can fairly say the y-axis up movement applies.

However, the consequence of peak shift within the filled samples does have a linear correlation for studied samples, in contradiction to Z_{eq} consequence shown in Table 2.

This may be referred to the fact that *B* calculation procedure depends rather on (ANSI/ANS-6.4.3-1991) parameter tables.

In addition to that, for the group of Figs. 3, *b*; 4, *b*; 5, *b* and 6, *b* concerning EABF, we can recognize a little bit of difference in progression either in the x-axis or y-axis directions. This could be explained according to the un-match between (ANSI/ANS-6.4.3-1991) for EBF and EABF parameter tables.

3.3 Kerma

The variation of kerma relative to air for the four samples at photons energy 1 keV - 20 MeV is illustrated in Fig. 7.

The K_a variation with photons energy represents the fluctuation in Z_{eq}. We can find the highest K_a values for S14 and the lowest for S1 since kerma depends on the sum of kinetic energies released primarily through partial interaction processes (photoelectric absorption, Compton scattering, and pair production in addition to others of less significance). S14 shows the highest curve according to its highest Fe content while S5 is slightly followed S9 due to their close percentages.

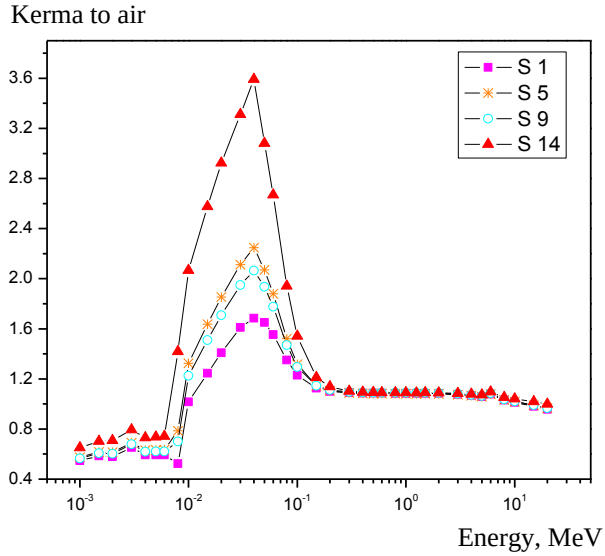

Fig. 7. The variation of kerma relative to the air of WP samples vs photon energy. (See color Figure on the journal website.)

The blank sample shows the least K_a and the filled one returns the highest K_a according to Z_{eq} values. A sharp peak exists at nearly 0.4 MeV. This peak could be due to the presence of Fe and other heavy elements in the filled samples since large pho-

ton interaction occurs for high Z elements where the photoelectric cross-section is proportional to Z by high magnitude.

4. Conclusion

The following conclusions could be drawn from the present study:

The values of the equivalent atomic number of the investigated samples show some relevance, in terms of filled and unfilled samples, to the atomic number of such materials' constituent elements, with little fluctuation over selected energies according to the Compton scattering reaction. Maximum values are for the filled S14 sample while the minimum is for the blank sample S1.

It is clear that sample S14 shows the least EBF and EABF among all samples over the concerned energy range with few variations, which means the high atomic number, in terms of iron, at S14 will compensate for higher thicknesses (thus cost on large production scales) required by other samples.

Further, the calculated kerma relative to air values for the investigated samples is useful in monitoring radiation dosimetry for γ-rays leaking behind such shields.

In the case of radioactive rubble, the leaking γ-radiation can be of different energy ranges, which requires multi-layer structure samples.

According to this study, obtained data could be useful and further investigations for buildup factors for multi-layered structures are required to be carried out.

REFERENCES

1. International Experts' Meeting on Decommissioning and Remediation after a Nuclear Accident. Vienna, Austria 28 Jan. - 1 Feb. 2013. IAEA-CN-211, (ID: 44453) (Vienna, IAEA, 2013) p. 59.
2. M.A.A. El-Sarraf, A. El-Sayed Abdo. Waste paper and natural rubber composite for radiation attenuation and radioactive debris shielding. Journal of Nuclear Research and Development 9 (2015) 56.
3. M. Madani et al. Utilization of waste paper in the manufacture of natural rubber composite for radiation shielding. Progress in Rubber. Plastics and Recycling Technology 20(4) (2004) 287.
4. S.E. Gwaily et al. Study of electrophysical characteristics of lead-natural rubber composites as radiation shields. Polymer Composites 23(6) (2002) 1068.
5. Gamma-Ray Attenuation Coefficients and Buildup Factors for Engineering Materials. American National Standard (ANSI/ANS 6.4.3., 1991).
6. N.A.M. Alsaif et al. Simulating the γ-ray and neutron attenuation properties of lithium borate glasses doped barite: efficient and deterministic analysis using relevant simulation codes. Journal of Materials Research and Technology 17 (2022) 679.
7. N.A.M. Alsaif et al. Calculating photon buildup factors in determining the γ-ray shielding effectiveness of some materials susceptible to be used for the conception of neutrons and γ-ray shielding. Journal of Materials Research and Technology 11 (2021) 769.
8. U. Kaur et al. Comparative studies of different concretes on the basis of some photon interaction parameters. Applied Radiation and Isotopes 70 (2012) 233.
9. *Reactor Shielding for Nuclear Engineer*. N.M. Schaeffer (Ed.) TID-25951 (U.S. Atomic Energy Commission, 1973) 800 p.
10. H. Akyildirim et al. Investigation of buildup factor in gamma-ray measurement. Acta Physica Polonica A 132(3-II) (2017) 1203.
11. S. Singh et al. Buildup of gamma ray photons in flyash concretes: A Study. Annals of Nuclear Energy 37 (5) (2010) 681.
12. M. Guvendik. Buildup factor formulae for multilayer shields. PhD Thesis (USA, Rolla, Missouri University of Science and Technology, 1999).
13. M.J. Berger et al. XCOM: Photon Cross Sections Database. NIST Standard Reference Database 8 (XGAM). (2010).
14. L. Gerward et al. X-ray absorption in matter. Reengineering XCOM. Radiation Physics and Chemistry 60 (2001) 23.
15. M. Kurudirek et al. Investigation of X- and gamma ray photons buildup in some neutron shielding materials using gp fitting approximation. Annals of Nuclear Energy 53 (2013) 485.
16. Y. Harima. An Approximation of Gamma-Ray Buildup Factors by Modified Geometrical Progression. Nucl. Sci. Eng. 83 (1983) 299.
17. Y. Harima. An Historical Review and Current Status of Buildup Factor Calculations and Applications. Radiation Physics and Chemistry 41 (1993) 631.
18. Y. Harima et al. Validity of the Geometric-Progression Formula in Approximating Gamma-Ray Buildup Factors. Nucl. Sci. Eng. 94 (1986) 24.
19. Y. Sakamoto, S. Tanaka, Y. Harima. Interpolation of Gamma-Ray Buildup Factors for Point Isotropic Source with Respect to Atomic Number. Nucl. Sci. Eng. 100 (1988) 33.
20. A. Shimizu. Calculations of Gamma-Ray Buildup Factors up to Depths of 100 mfp by the Method of Invariant Embedding, (I) Analysis of Accuracy and Comparison with Other Data. Journal of Nuclear Science and Technology 39 (2002) 477.
21. A. Shimizu, T. Onda, Y. Sakamoto. Calculations of Gamma-Ray Buildup Factors up to Depths of 100 mfp by the Method of Invariant Embedding, (III) Generation of an Improved Data Set. Journal of Nuclear Science and Technology 41 (2004) 413.
22. M. Almatari. Energy Absorption and Exposure Buildup Factors for Some Bioactive Glasses Samples: Penetration Depth, Photon Energy, and Atomic Number Dependence. Journal of Optoelectronics and Biomedical Materials 9(2) (2017) 95.

23. K.S. Mann et al. Investigations of some building materials for γ-rays shielding effectiveness. Radiation Physics and Chemistry 87 (2013) 16.
24. S.R. Manohara, S.M. Hanagodimath, L. Gerward. Studies on effective atomic number, electron density and kerma for some fatty acids and carbohydrates. Phys. Med. Biol. 53 (2008) 377.
25. K.S. Mann, M. Kurudirek, G.S. Sidhu. Verification of dosimetric materials to be used as tissue-substitutes in radiological diagnosis. Applied Radiation and Isotopes 70 (2012) 681.
26. P.S. Singh, T. Singh, P. Kaur. Variation of energy absorption buildup factors with incident photon energy and penetration depth for some commonly used solvents. Ann. Nucl. Energy 35 (2008) 1093.
27. T. Singh, N. Kumar, P.S. Singh. Chemical composition dependence of exposure buildup factors for some polymers. Ann. Nucl. Energy 36 (2009) 114.
28. M. Kurudirek, Y. Özdemir. A comprehensive study on energy absorption and exposure buildup factors for some essential amino acids, fatty acids and carbohydrates in the energy range 0.015 - 15 MeV up to 40 mean free path. Nuclear Instruments and Methods in Physics Research B 269 (2011) 7.
29. F.H. Attix. *Introduction to Radiological Physics and Radiation Dosimetry*. 1st ed. (Wiley-VCH, 1991) 628 p.
30. Radiation Quantities and Units. ICRU Report 33 (Bethesda, USA, 1980).
31. J.H. Hubbell, S.M. Seltzer. *Tables of X-Ray Mass Attenuation Coefficients and Mass Energy-Absorption Coefficients 1 keV to 20 MeV for Elements Z = 1 to 92 and 48 Additional Substances of Dosimetric Interest*. NISTIR-5632 (Gaithersburg, USA, 1995) 120 p.

М. А. Ель-Сарраф[1,*], А. А. Ель-Саїд Абдо[2]

[1] Центр досліджень ядерної та радіологічної безпеки, Управління атомної енергії Єгипту, Каїр, Єгипет
[2]Центр ядерних досліджень, Управління атомної енергії Єгипту, Каїр, Єгипет

*Відповідальний автор: magdsarraf@yahoo.com

ОЦІНКА ПАРАМЕТРІВ ДЛЯ РОЗРАХУНКІВ ЕНЕРГОВИДІЛЕННЯ ВІД ГАММА-КВАНТІВ У ДЕЯКИХ КОМПОЗИТНИХ МАТЕРІАЛАХ

У даній роботі досліджено декілька параметрів, що характеризують енерговиділення від фотонів в області енергій від 0,015 до 15,0 МеВ для чотирьох композитів з використаного паперу. Для захисту від радіоактивних уламків у різний час використовувалися композити з макулатури та натурального каучуку (WP/NR) різної щільності в діапазоні від ρ = 0,894 до 1,16 гм·см$^{-3}$. Також використовувалися деякі добавки, включаючи сажу з високою абразивністю, парафін, B_4C, а також магнетит. Отримані параметри взаємодії фотонів: еквівалентний атомний номер Z_{eq}, коефіцієнти накопичення для експозиції та енергії поглинання були вивчені залежно від енергії гамма-кванта, елементного складу WP/NR та для глибини проникнення до 40 середніх довжин вільного пробігу. Значення Z_{eq} показали незначну варіацію у вибраному діапазоні енергій, а коефіцієнти накопичення виявилися невеликими при низькій і високій енергіях, при великих значеннях у проміжній енергетичній області. Крім того, було обчислено керму відносно повітря для енергій гамма-квантів від 1 до 20 МеВ і показано її залежність від еквівалентних атомних номерів. У роботі було продемонстровано, що заповнені зразки пропонують кращі можливості для екранування, ніж незаповнені. Отримані дані можуть бути корисні в радіаційній фізиці при оцінці γ-радіації після WP/NR екранів.

Ключові слова: композити, коефіцієнти накопичення, експозиція, енергопоглинання, керма.

Надійшла/Received 20.06.2022